Reaction of Cytochrome P450 with Cumene Hydroperoxide: ESR Spin-Trapping Evidence for the Homolytic Scission of the Peroxide O–O Bond by Ferric Cytochrome P450 1A2

ARTICLE *in* CHEMICAL RESEARCH IN TOXICOLOGY · JANUARY 1996

Impact Factor: 3.53 · DOI: 10.1021/tx9501501 · Source: PubMed

Reaction of Cytochrome P450 with Cumene Hydroperoxide: ESR Spin-Trapping Evidence for the Homolytic Scission of the Peroxide O−O Bond by Ferric Cytochrome P450 1A2

David P. Barr,*,† Martha V. Martin,‡ F. Peter Guengerich,‡ and Ronald P. Mason†

Laboratory of Molecular Biophysics, National Institute of Environmental Health Sciences, National Institutes of Health, Research Triangle Park, North Carolina 27709, and Department of Biochemistry and Center in Molecular Toxicology, Vanderbilt University, Nashville Tennessee 37232-0146

Received August 25, 1995[⊗]

ESR spin trapping was used to investigate the reaction of rabbit cytochrome P450 (P450) 1A2 with cumene hydroperoxide. Cumene hydroperoxide-derived peroxyl, alkoxyl, and carbon-centered radicals were formed and trapped during the reaction. The relative contributions of each radical adduct to the composite ESR spectrum were influenced by the concentration of the spin trap. Computer simulation of the experimental data obtained at various 5,5-dimethyl-1-pyrroline *N*-oxide (DMPO) concentrations was used to quantitate the contributions of each radical adduct to the composite ESR spectrum. The alkoxyl radical was the initial radical produced during the reaction. Experiments with 2-methyl-2-nitrosopropane identified the carbon-centered adducts as those of the methyl radical, hydroxymethyl radical, and a secondary carbon-centered radical. The reaction did not require NADPH-cytochrome P450 reductase or NADPH. It is concluded that the reaction involves the initial homolytic scission of the peroxide O−O bond to produce the cumoxyl radical. Methyl radicals were produced from the β-scission of the cumoxyl radical. The peroxyl adduct was not observed in the absence of molecular oxygen. We conclude that the DMPO peroxyl radical adduct detected in the presence of oxygen was due to the methylperoxyl radical formed by the reaction of the methyl radical with oxygen. At a higher P450 concentration, a protein-derived radical adduct was also detected.

Introduction

Organic hydroperoxides have provided great utility in elucidating the mechanism of oxygen activation by cytochrome P450 (P450).[1] The peroxide-dependent pathway, also known as the "peroxide shunt", was described by Hrycay and O'Brien (*1*) and Kadlubar et al. (*2*) in the early 1970s. Subsequently, it was found that cumene hydroperoxide could support several P450-catalyzed reactions including aromatic and aliphatic hydroxylation, N- or O-dealkylation, and alkene epoxidation (*3*−*5*). The mechanism involves the formation of a reactive, oxene-like or perferryl intermediate which catalyzes the insertion of oxygen into the substrate via an "oxygen rebound" mechanism (*6*, *7*). It is agreed that the oxidation equivalents for this reaction are derived from the scission of the peroxide O−O bond, but there has been some controversy as to whether the bond is cleaved heterolytically or homolytically (*8*−*13*). Recent evidence suggests that P450 may catalyze both heterolysis and homolysis (*14*−*17*). The two possible mechanisms for peroxide reduction are illustrated below.

heterolytic

$$\text{P450-Fe}^{\text{III}} + \text{ROOH} \rightarrow \text{P450}^{\bullet+}(\text{Fe}^{\text{IV}}{=}\text{O}) + \text{ROH} \quad (1)$$

homolytic

$$\text{P450-Fe}^{\text{III}} + \text{ROOH} \rightarrow \text{P450}\,(\text{Fe}^{\text{IV}}{=}\text{O}) + \text{RO}^{\bullet} + \text{H}^{+} \quad (2)$$

Organic peroxides are also used in various industrial processes and are known tumor promoters (*18*). Thus, the metabolism of organic peroxides is of importance from a toxicological standpoint. Most of the studies have focused on their ability to promote tumorogenesis in skin (*18*). The mechanism by which organic peroxides exert their tumorogenic effect has been the topic of recent investigations and is thought to involve heme protein-catalyzed free-radical production (*19*). Davies and coworkers (*20*, *21*) used ESR spin trapping to demonstrate the production of free radicals from the reaction of organic hydroperoxides with rat liver microsomal preparations. In such studies, the radicals react with a nitrone or nitroso compound to form a relatively stable, ESR-detectable radical adduct. Analysis of the characteristic nitrogen and hydrogen hyperfine coupling constants of these radical adducts allows one to identify the radicals produced in the initial reaction. Both peroxyl and carbon-centered radical adducts were detected in the studies using rat liver microsomes (*20*). It was proposed that the radicals were formed via the homolytic reduction of the peroxide by ferrous P450. Thus, it was implied that NADPH and P450 reductase were required for

† NIH.
‡ Vanderbilt University.
[⊗] Abstract published in *Advance ACS Abstracts,* December 15, 1995.
[1] Abbreviations: P450, cytochrome P450; DMPO, 5,5-dimethyl-1-pyrroline *N*-oxide; DTPA diethylenetriaminepentaacetic acid; SOD, superoxide dismutase; CumOOH, cumene hydroperoxide; CumOO•, cumyl peroxyl radical; CumO•, cumoxyl radical; MNP, 2-methyl-2-nitrosopropane.

0893-228x/96/2709-0318$12.00/0

homolysis to occur. This mechanism of homolytic peroxide bond cleavage was in contrast to that proposed by others which did not involve ferrous P450 (*9*, *10*, *12*).

Previous studies have suggested that several heme proteins (including P450) produce radicals from hydroperoxides via a peroxidase-type mechanism (*20*−*23*). This would initially involve the heterolytic reduction of the hydroperoxide (reaction 1). Subsequent hydrogen abstraction from another molecule of hydroperoxide by the ferryl radical form of the heme protein (i.e., compound I) would produce a peroxyl radical. This mechanism seemed plausible, since free-radical reactions forming secondary radicals can be used to explain the production of the alkoxyl and carbon-centered radical adducts that were detected. However, we recently found that cytochrome *c* catalyzed the homolytic cleavage of cumene hydroperoxide to initially produce an alkoxyl radical (*24*). In contrast to previous interpretations, the peroxyl radical, and not the alkoxyl radical, was found to be the result of radical chemistry. Here, we have investigated the reaction of purified P450 1A2 with cumene hydroperoxide using ESR spin trapping, with the intent of elucidating the mechanism of radical production. The implications of these data with regard to hydroperoxide metabolism by P450 and its toxicological relevance are discussed.

Materials and Methods

Chemicals. Cytochrome P450 1A2 was purified from rabbit hepatic microsomes (5,6-benzoflavone-treated rabbits) as described in refs 25 and 26. Cumene hydroperoxide and MNP were purchased from Aldrich (Milwaukee, WI). The cumene hydroperoxide was purified by preparing the sodium salt as described by Mair and Hall (*27*). The DMPO was obtained from the Oklahoma Medical Research Foundation (Oklahoma City, OK) and was vacuum distilled twice at room temperature before use. Sodium phosphate and DTPA were purchased from Sigma (St. Louis, MO). Glucose oxidase and superoxide dismutase were obtained from Boehringer-Mannheim (Indianapolis, IN). The reagents and buffer were prepared using deionized water and were treated with Chelex 100 (Bio-Rad, Hercules, CA).

ESR Spin-Trapping Experiments. ESR spectra were recorded using a Bruker ECS-106 spectrometer (Billerica, MA) operating at 9.77 GHz with a modulation frequency of 50 kHz and a TM_{110} cavity. The reactions were initiated by the addition of cumene hydroperoxide and were pipetted into the flat cell. The time delay before recording spectra was ~1.5 min. For the experiments shown in Figures 4 and 6, glucose and glucose oxidase were added to the reaction mixture 3 min before the addition of P450 to produce anaerobic conditions. For the experiment shown in Figure 4 the solution containing all reactants except P450 was bubbled with N_2 for 5 min prior to the addition of glucose and glucose oxidase. The reactions were all performed in 100 mM sodium phosphate solutions, pH 7.4, that also contained 200 μM DTPA to prevent possible trace transition metal catalysis.

Computer Simulations. The computer simulations were performed using a program that is available to the public through the Internet (http://alfred.niehs.nih/LMB). The details of the program were described in a recent publication (*28*). The parameters that were used for simulating each species are described in the figure legends. The data points in Figure 3 were obtained by simulating the low-field lines of each species at the various DMPO concentrations. The experiments were also performed in the absence of P450 at each DMPO concentration. The background signals obtained in the absence of P450 were subtracted from those obtained in its presence. The simulated data were then double integrated to determine the relative concentrations of each radical adduct.

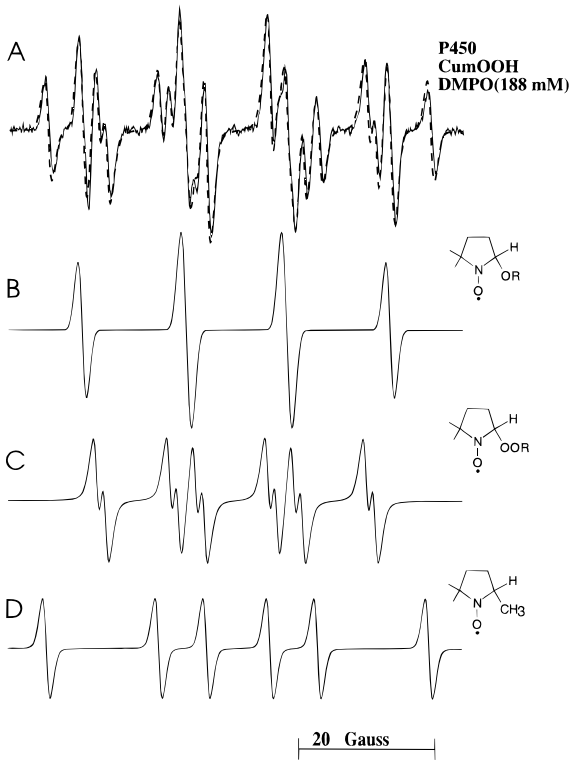

Figure 1. Computer simulation and deconvolution of the ESR spectrum obtained from the reaction of cumene hydroperoxide with P450 1A2. (A) is the computer simulation (dashed line) superimposed on the experimental spectrum obtained using 4 μM P450, 12.5 mM cumene hydroperoxide, and 188 mM DMPO. (B−D) are the individual simulations of each species in the composite spectrum. The hyperfine values for each species are provided under Results. (B) is the simulated spectrum for DMPO/•OR: line width, 0.65 G; line shape, 0% Lorentzian and 100% Gaussian; and mole ratio, 0.26. (C) is the simulated spectrum for DMPO/•OOR: line width, 0.75 G; line shape, 73% Lorentzian and 27% Gaussian; and mole fraction, 0.57. (D) is the simulated spectrum for the DMPO/carbon-centered radical: line width, 0.65 G; line shape, 45% Lorentzian and 55% Gaussian; and mole fraction, 0.17. Spectrometer conditions: microwave power, 20 mW; modulation amplitude, 0.5 G; time constant, 0.69 s; scan time, 600 s; scan range, 80 G; receiver gain, 2.5×10^5.

Results

A mixture of three radical adducts was detected from the reaction of rabbit P450 1A2 with cumene hydroperoxide in the presence of DMPO (Figure 1). The spectrum was similar to what was observed in earlier studies from the reaction of other heme proteins with cumene hydroperoxide (*22*). The computer simulation used to obtain the hyperfine coupling constants was superimposed on the experimental spectrum (Figure 1A), and the adducts were assigned as follows: methylperoxyl (a^N = 14.5 G, a_β^H = 10.75 G, and a_γ^H = 1.30 G) (see below), carbon-centered (a^N = 16.4 G and a_β^H = 23.5 G), and cumoxyl (a^N = 14.8 G and a_β^H = 15.8 G). The hyperfine values were consistent with previously reported values for these adducts (*22*). Parts B−D of Figure 1 are simulations of the individual radical adducts which were obtained using the hyperfine values and relative intensities from the composite simulation.

There are several radical reactions that can occur subsequent to the production of the initial radical by P450 and can be used to account for the radical adducts seen in Figure 1 (*vide infra*). However, such an experiment (as summarized in Figure 1) cannot be used to

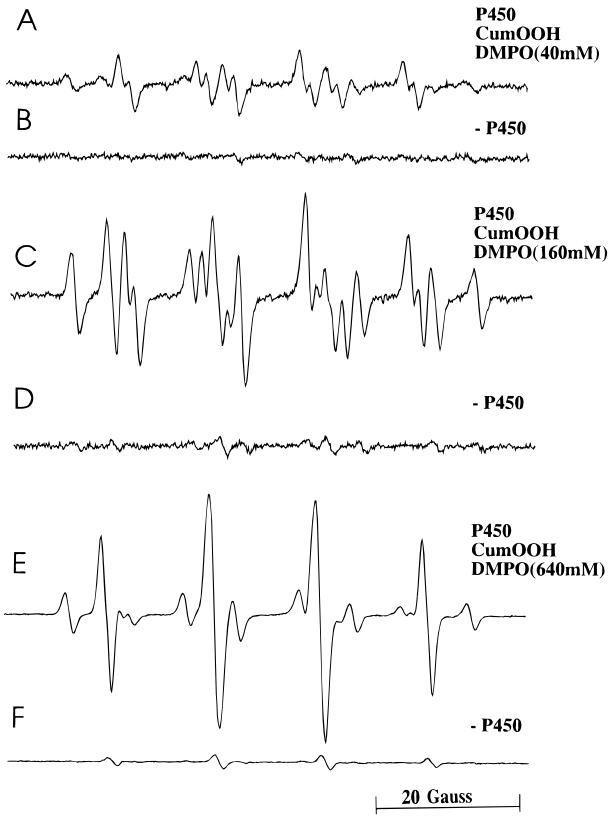

Figure 2. Composite ESR spectrum of DMPO adducts from the incubations of P450 1A2 with cumene hydroperoxide at various DMPO concentrations. (A) is the ESR signal obtained from a reaction mixture containing 4 μM P450, 12.5 mM cumene hydroperoxide, and 40 mM DMPO. (B) is the spectrum obtained using the conditions from (A), except P450 was omitted. (C) is the ESR signal obtained from a reaction mixture containing 4 μM P450, 12.5 mM cumene hydroperoxide, and 160 mM DMPO. (D) is the spectrum obtained using the conditions from (C), except P450 was omitted. (E) is the ESR signal obtained from a reaction mixture containing 4 μM P450, 12.5 mM cumene hydroperoxide, and 640 mM DMPO. (F) is the spectrum obtained using the conditions from (E), except P450 was omitted. The spectrometer conditions were the same as described in Figure 1, except a time constant of 0.33 s and a scan time of 335 s were used.

determine whether an alkoxyl or a peroxyl radical is formed initially. In a previous study we were able to determine the initial radical produced from the reaction of cytochrome *c* with cumene hydroperoxide by varying the DMPO concentration (*24*). Radical reactions that occur subsequent to the production of the initial radical can be suppressed by increasing the concentration of the spin trap. Therefore, the formation of the adduct that corresponds to the initial radical will increase as the spin trap is increased, and those adducts that depend upon the subsequent reactions of the initial radical will decrease. When the concentration of DMPO was increased, the relative intensity of the peroxyl radical adduct decreased while that of the cumoxyl radical adduct increased (Figure 2). In the absence of P450, a weak ESR signal could be seen at the higher DMPO concentrations (Figure 2D,F). This signal is due to DMPO/hydroxyl radical adduct that is present as a contaminant in the DMPO preparation. Although the DMPO was vacuum distilled twice before use, some of this contaminant remained and could be detected at high DMPO concentrations. The experiment was performed at several DMPO concentrations (Figure 3), and the relative concentrations of each radical adduct were determined using double integration. Before quantitation, the background signal from each DMPO concentration (obtained in the absence of P450) was subtracted from the spectrum obtained in the presence of P450. As the DMPO concentration was increased from 20 to 1800 mM, the contribution of the peroxyl adduct to the composite spectrum decreased from ~90% to less than 15%. Meanwhile, the contribution of the cumoxyl adduct increased over this range from less than 10% to ~80%. The effect of the DMPO concentration on the methyl radical adduct contribution was less marked but increased slightly from 20 mM DMPO to 640 mM and decreased between 640 and 1800 mM. It did not appear that DMPO caused denaturation of P450 (i.e., conversion to P420) even at high concentrations. Instead, we found that DMPO formed a type II binding complex with P450 1A2 (as determined by difference spectroscopy) and had an absorption minimum at 392 nm and a maximum at 431 nm (data not shown). Augusto et al. (*29*) reported an apparent K_s of 6.1 mM for the DMPO/P450 type II complex using rat liver microsomes. However, using purified 1A2 and our experimental conditions, we found the apparent K_s to be 1.7 M (data not shown). Because of this low affinity of DMPO for P450 1A2, we do not believe that DMPO could have competed effectively with cumene hydroperoxide for heme iron coordination and, thus, did not interfere with our experimental results.

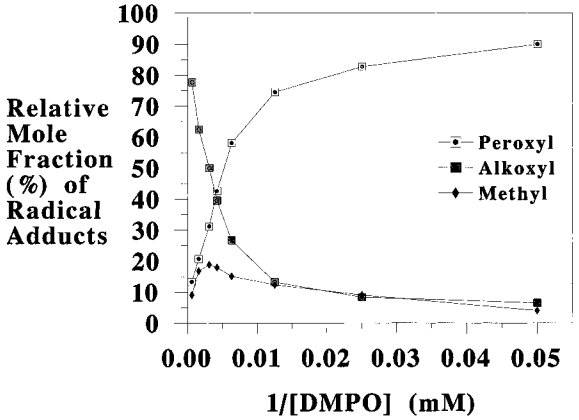

Figure 3. Effect of the DMPO concentration on the relative contributions of each radical adduct to the composite spectrum obtained from the reaction of P450 1A2 with cumene hydroperoxide. All reaction mixtures contained 4 μM P450, 12.5 mM cumene hydroperoxide, and 100 mM phosphate buffer with 200 μM DTPA. DMPO concentrations used: 20, 40, 80, 160, 240, 320, 640, and 1800 mM. ⊡, DMPO/$^{\bullet}$OOR; ■, DMPO/$^{\bullet}$OR; ◆, DMPO/$^{\bullet}$CR$_3$.

The data in Figure 3 demonstrated that the peroxyl radical cannot be the radical initially produced by P450. However, any of the reactions 3−5 could account for the

$$^{\bullet}CH_3 + O_2 \rightarrow {}^{\bullet}OOCH_3 \quad (3)$$

$$CumO^{\bullet} + CumOOH \rightarrow CumOH + CumOO^{\bullet} \quad (4)$$

$$^{\bullet}CH_3 + CumOOH \rightarrow CH_4 + CumOO^{\bullet} \quad (5)$$

peroxyl radical adduct that was detected at the lower DMPO concentrations. These reactions are all valid possibilities, as the ESR spectra of the DMPO adducts of tertiary and primary peroxyl radicals are very similar. We were able to evaluate the contribution of (3) by performing the reaction in the presence or absence of oxygen. Removing molecular oxygen resulted in the loss of almost all of the peroxyl radical adduct (Figure 4). An

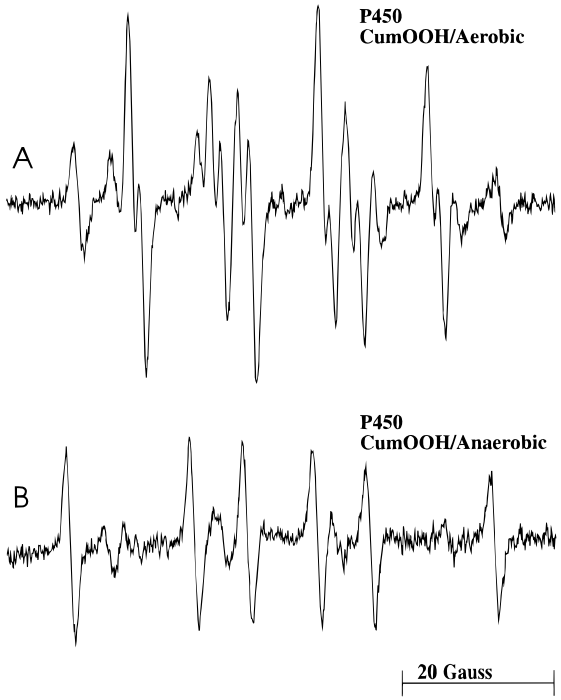

Figure 4. Effect of oxygen on the production of DMPO radical adducts from the reaction of P450 1A2 with cumene hydroperoxide. (A) is the spectrum obtained in the presence of oxygen from a reaction mixture containing 4 μM P450, 12.5 mM cumene hydroperoxide, and 40 mM DMPO under aerobic conditions. (B) is the spectrum obtained using the conditions from (A), except that the system was anaerobic. The reaction was depleted of oxygen by first bubbling the solution with N_2 for 5 min. Glucose oxidase (100 units) and glucose (15 mM) were added to the reaction mixture 3 min before the addition of P450.

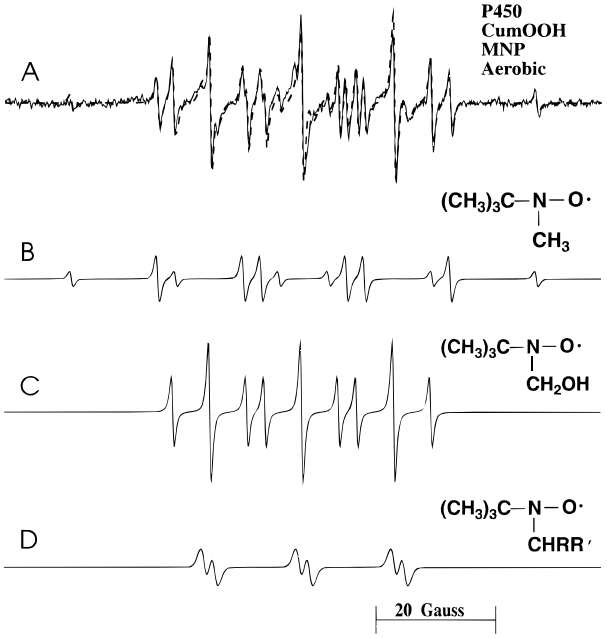

Figure 5. Computer simulation and deconvolution of the ESR spectrum obtained from the reaction mixture containing P450 1A2, cumene hydroperoxide, and MNP under aerobic conditions. (A) is the computer simulation (dashed line) superimposed on the experimental spectrum obtained using 4 μM P450, 12.5 mM cumene hydroperoxide, and 18 mM MNP. (B−D) are the individual simulations for each species in the composite spectrum. The hyperfine values are provided under Results. (B) is the simulated spectrum for MNP/•CH_3: line width, 0.45 G; line shape, 71% Lorentzian and 29% Gaussian; and mole fraction, 0.24. (C) is the simulated spectrum for MNP/•CH_2OH: line width, 0.45 G; line shape, 100% Lorentzian and 0% Gaussian; and mole fraction, 0.52. (D) is the simulated spectrum for MNP/•CHRR′ (secondary carbon): line width, 0.70; line shape, 30% Lorentzian and 70% Gaussian, and mole fraction, 0.24. Spectrometer conditions: microwave power, 20 mW; modulation amplitude, 0.5 G; time constant, 0.69 s; scan time, 600 s; scan range, 100 G; receiver gain, 2.5×10^5.

increase in the ESR signal of the carbon-centered adduct was observed concomitantly with the decrease in the peroxyl radical adduct. Also, superoxide dismutase had no effect on the ESR signals detected, excluding a contribution from DMPO/superoxide (data not shown). Thus, it appeared likely that the peroxyl radical signal was that of the methylperoxyl radical formed via reaction 3.

The carbon-centered radicals formed during the reaction of P450 with cumene hydroperoxide were further characterized using the nitroso spin trap MNP. With nitroso spin traps, the radical adds directly to the nitroxide nitrogen. Therefore, these adducts are more informative with regard to the type of carbon-centered radical that has been trapped (e.g., methyl, primary, secondary or tertiary carbon). Three radical adducts were detected from the reaction of cumene hydroperoxide with P450 (Figure 5). These were assigned as follows: methyl (a^N = 17.4 G and a_β^H = 14.4 G (3H)), hydroxymethyl (a^N = 15.5 G and a_β^H = 6.2 G (2H)), and RĊHR′ (a^N = 15.1 G and a_β^H = 1.7 G (1H)). The hyperfine values for the methyl and hydroxymethyl MNP adducts were similar to those reported by Chamulitrat et al. (*22*) from the reaction of chloroperoxidase with cumene hydroperoxide. The third MNP adduct, represented by a six-line spectrum (Figure 5D), was due to a carbon-centered radical with only one β-hydrogen. The types of adducts formed with MNP were also influenced by oxygen. In the absence of oxygen, the intensity of the signal corresponding to the methyl radical adduct was greatly increased while that for the hydroxymethyl adduct was not detected (Figure 6). Instead, another nine-line spectrum consisting of three triplets with 1:2:1 intensity was detected (Figure 6). This adduct had hyperfine splitting values identical to the ethyl radical adduct of MNP (a^N = 17.0 G, a_β^H = 11.1 G (2H)) that was reported previously and was explained by the double trapping of the methyl radical (*19*, *22*). The radical adduct corresponding to the carbon-centered radical with one β-hydrogen was also detected in the absence of oxygen (Figure 6D).

The concentration of P450 also had an effect on the ESR spectrum observed with MNP. Figure 7A shows the spectrum when 4 μM P450 was used. In the absence of P450, no signal was observed (Figure 7B). When the concentration of P450 was raised from 4 to 25 μM, the spectrum from a strongly immobilized nitroxide was detected (Figure 7C). This immobilized spectrum was evidently due to a radical center localized on the protein. The isotropic lines from the carbon-centered adducts described in Figure 6 can also be seen. The features of this immobilized nitroxide became more prominent when the modulation amplitude was increased (Figure 7D), and a splitting of ~61 Gauss was measured between the low-field maximum and the high-field minimum (i.e., $2a_{||}^N$).

Discussion

Over the last two and a half decades, extensive studies have been performed to elucidate the mechanism of hydroperoxide-supported, P450-catalyzed reactions. Evidence for two mechanisms of hydroperoxide reduction has

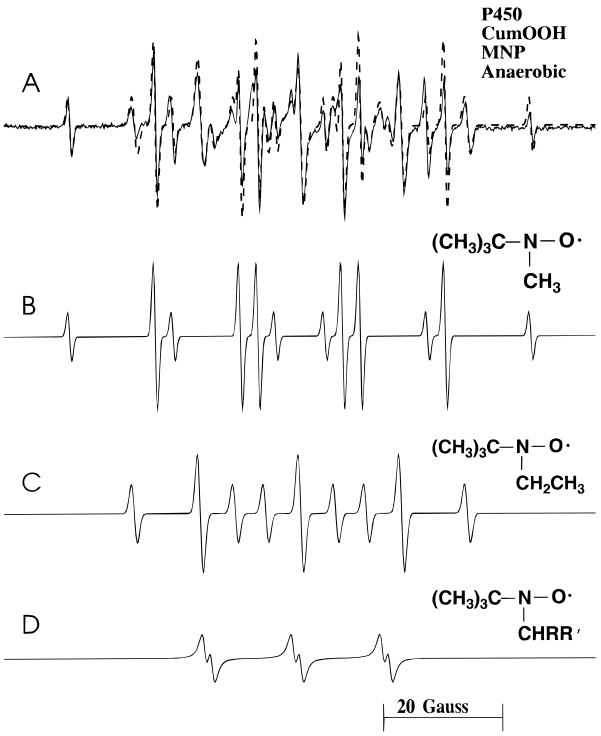

Figure 6. Computer simulation and deconvolution of the ESR spectrum obtained from the reaction mixture containing P450 1A2, cumene hydroperoxide, and MNP under anaerobic conditions. (A) is the computer simulation (dashed line) superimposed on the experimental spectrum obtained using 4 μM P450, 12.5 mM cumene hydroperoxide, 18 mM MNP, and anaerobic reaction conditions. The solution was made anaerobic before initiating the reaction as was described in Figure 4, except the solution was not bubbled with N_2 due to the volatility of MNP. (B−D) are the individual simulations for each species in the composite spectrum. The hyperfine values are provided under Results. (B) is the simulated spectrum for MNP/$^{\bullet}CH_3$: line width, 0.35 G; line shape, 0% Lorentzian and 100% Gaussian; and mole fraction, 0.32. (C) is the simulated spectrum for MNP/$^{\bullet}CH_2$-CH_3: line width, 0.50 G; line shape, 0% Lorentzian and 100% Gaussian; and mole fraction, 0.33. (D) is the simulated spectrum for MNP/$^{\bullet}$CHRR′ (secondary carbon): line width, 0.85; line shape, 100% Lorentzian and 0% Gaussian, and mole fraction, 0.36. Spectrometer conditions: microwave power, 20 mW; modulation amplitude, 0.5 G; time constant, 0.69 s; scan time, 600 s; scan range, 100 G; receiver gain, 2.5×10^5.

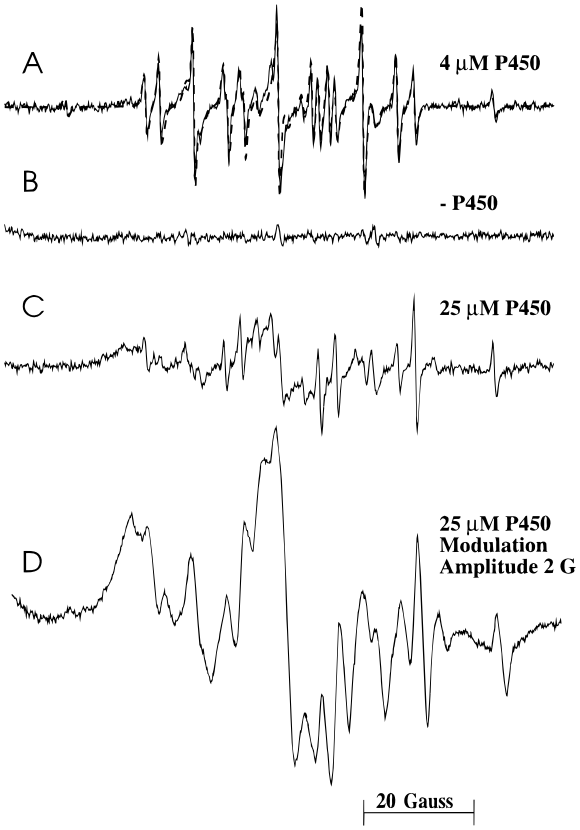

Figure 7. Effect of the P450 concentration on the MNP radical adduct ESR spectrum. (A) is the spectrum obtained from using 4 μM P450, 12.5 mM cumene hydroperoxide, and 18 mM MNP. (B) is the spectrum obtained using the conditions from (A), except P450 was omitted. (C) is the spectrum obtained using the conditions from (A), except 25 μM P450 was used. (D) is the spectrum obtained using the conditions from (B), except the modulation amplitude was increased to 2 G. The spectrometer conditions were the same as described in Figure 5.

been compiled in numerous reports (*3*−*17*). The first mechanism involves the two-electron reduction of the peroxide followed by heterolysis of the O−O bond (reaction 1). This would imply that the initial products formed are an alcohol and a ferryl cation radical form of P450. Such an intermediate would be analogous to the oxene, compound I species of a peroxidase formed during heterolysis of hydrogen peroxide. It is this P450 intermediate that is thought to initiate the wide variety of hydroxylation and dealkylation reactions that have been reported for the P450/hydroperoxide system. In fact, ^{18}O-labeling experiments have demonstrated that the peroxide oxygen is incorporated into the substrate during the hydroxylation reaction (*10*).

The homolytic cleavage mechanism (reaction 2) has also been well documented (*9*−*12*, *16*). For example, the detection of products such as acetophenone and methane from the reaction of P450 with cumene hydroperoxide can be most easily explained by a mechanism that involves the initial homolysis of cumene hydroperoxide to the cumoxyl radical. Subsequent β-scission of the cumoxyl radical would yield the methyl radical and acetophenone.

More recently, evidence has been obtained that suggests P450 might initiate both heterolytic and homolytic cleavage of peroxides. Lee and Bruice (*15*) demonstrated that a synthetic iron porphyrin could perform both homolytic and heterolytic cleavage of various peroxides and that the extent of heterolysis depended on the pK_a of the corresponding alcohol that is formed. Thompson and Yumibe (*16*) compared product ratios to evaluate the extent of heterolysis versus homolysis from the reaction of microsomes with various organic hydroperoxides, including cumene hydroperoxide. The extent of homolysis seemed to depend on the stability of the carbon radical that was liberated following β-scission of the alkoxyl radical. Thus, a phenyl substitution in the β-position resulted in a greater proportion of the hydroperoxide undergoing homolytic cleavage. Shimizu et al. (*14*) demonstrated that the mutation of Glu^{318} or Thr^{319} in rat P450 1A2 affected whether a compound I "type" (indicating heterolysis) or a compound II "type" (indicating homolysis) absorbance spectrum was observed following the reaction of the protein with cumene or *tert*-butyl hydroperoxide. Correia et al. (*17*) studied the products formed from reactions of peroxyquinols with either purified P450s or microsomes obtained from animals treated with various P450-inducing agents. They concluded that there was a difference in the ratio of heterolytic to homolytic cleavage that depended on the P450 enzyme used.

Sufficient evidence has been reported to support the view that P450 can catalyze both heterolytic and ho-

molytic peroxide bond cleavage. While heterolytic cleavage may better explain the mechanism by which substrates are hydroxylated by P450, the homolytic mechanism provides a mode of activation that would account for the production of free radicals and, thus, the cytotoxic action of organic hydroperoxides.

Recently, Davies and co-workers have proposed that alkoxyl radical production by the P450/hydroperoxide system is dependent upon the presence of NADPH and P450 reductase (*20*). In their study, ESR spin trapping was used to detect the radicals formed in a system containing rat liver microsomes and various hydroperoxides (including cumene hydroperoxide). With DMPO as the spin trap and cumene as the hydroperoxide, only a carbon-centered adduct and the cumyl peroxyl radical adduct were detected. The carbon-centered adduct was identified as the methyl radical adduct using the nitroso spin trap 3,5-dibromo-4-nitrosobenzenesulfonic acid. It was reported that, with several hydroperoxides, NADPH was required to detect the methyl radical and that, in its absence, only the peroxyl radical adduct was detected. Therefore, it was concluded that NADPH and the reductase were required to reduce P450 to the ferrous form. Ferrous P450 would catalyze the homolytic cleavage of the peroxide O−O bond.

$$P450(Fe^{III}) + NADPH \xrightarrow{\text{P450 reductase}} P450(Fe^{II}) + NADP^{+} \quad (6)$$

$$P450(Fe^{II}) + CumOOH \rightarrow CumO^{\bullet} + P450(Fe^{III}) \quad (7)$$

In the absence of NADPH, only the peroxyl radical adduct was observed. The mechanism proposed for peroxyl radical formation involved the initial heterolytic scission of the O−O bond by ferric P450, followed by hydrogen abstraction from another molecule of hydroperoxide by a ferryl radical (compound I) form of P450.

$$P450(Fe^{III}) + CumOOH \rightarrow P450^{\bullet+}(Fe^{IV}{=}O) + CumOH \quad (8)$$

$$P450^{\bullet+}(Fe^{IV}{=}O) + CumOOH \rightarrow P450(Fe^{IV}{=}O) + CumOO^{\bullet} \quad (9)$$

Our spin-trapping results from the reaction of purified rabbit P450 1A2 with cumene hydroperoxide were quite different from those reported for rat liver microsomes, but support the conclusions made by Weiss and Estabrook (*9*) and Cavallini et al. (*30*). All of the experiments in the present study were performed in the absence of the reductase and NADPH, so radical production was independent of the ferrous form of the enzyme. In addition, bubbling the solution with CO had the same effect as bubbling the solution with N_2. In each case, the spectra recorded indicated that the system was anoxic (i.e., spectra were similar to Figure 4B) (data not shown). If ferrous P450 had been involved, CO would have been expected to attenuate the signals. When DMPO was used as the spin trap, a mixture of adducts was detected. These included the cumyl peroxyl adduct, the cumoxyl adduct, and carbon-centered adduct(s). The concentration of DMPO strongly influenced the proportion that each adduct contributed to the composite spectrum. In particular, the contribution of the cumoxyl adduct increased as the DMPO concentration was increased, while that of the cumyl peroxyl adduct decreased. As was mentioned earlier, radical reactions can be used to explain the formation of all of the radical adducts that were detected. In the case of the peroxidase-type mechanism, the cumyl peroxyl radical would be the initial radical formed (reaction 9). The self-reaction of tertiary peroxyl radicals is known to yield two cumoxyl radicals and molecular oxygen (*31*) (reaction 10). The well-

$$2CumOO^{\bullet} \rightarrow 2CumO^{\bullet} + O_2 \quad (10)$$

$$CumO^{\bullet} \rightarrow \text{acetophenone} + {}^{\bullet}CH_3 \quad (11)$$

established β-scission of the cumoxyl radical (reaction 11) would explain the detection of the methyl radical.

Thus, reactions 8−11 could be used to explain all of the radical adducts that were detected. However, one would expect that as the concentration of DMPO was increased, the cumyl peroxyl radical adduct would also have increased because the trapping of essentially all of the cumyl peroxyl radicals would occur at high concentrations of the spin trap and prevent reactions 10 and 11 from occurring. Since the cumoxyl radical adduct increased with increasing spin-trap concentration, we conclude that the cumoxyl radical, and not the cumyl peroxyl radical, must be the initial radical formed. This would imply that the peroxide was homolytically cleaved as shown in reaction 2. Reaction 11 would then account for the methyl radical. Although DMPO/peroxyl adducts have similar hyperfine values and, therefore, are difficult to distinguish, the peroxyl adduct seen in this study seems to be primarily that of the methylperoxyl radical. Very little peroxyl adduct was detected when the reaction was performed in the absence of oxygen. Instead, the signal intensity that was lost from the peroxyl adduct was gained in the methyl radical adduct. This phenomenon can easily be rationalized by considering reaction 3 as being responsible for the majority of the peroxyl adduct. We cannot rule out the possibility that some cumyl peroxyl radical adduct was formed, as the peroxyl adduct was not completely suppressed under anaerobic conditions. Superoxide dismutase also had no effect on the remaining peroxyl radical signal detected during the anaerobic reaction, nor did it affect the signals observed in the aerobic reaction. Therefore, the peroxyl adduct was not due to superoxide in either case. It should be noted that the hyperfine coupling constants for the DMPO methyloxyl adduct are similar to those of DMPO peroxyl adducts (*32*). Thus, the adduct we are assigning to the methylperoxyl adduct might be the methyloxyl adduct. In either case, the radical adduct would be derived from the methylperoxyl radical and would not change our mechanistic conclusions.

Experiments with MNP were performed to reveal the identity of the carbon-centered adducts that were detected with DMPO. This was necessary because the hyperfine splitting values of carbon-centered DMPO adducts are all relatively similar. In the presence of O_2, a spectrum was obtained that was very similar to that reported by Chamulitrat et al. (*22*) for the reaction of chloroperoxidase with cumene hydroperoxide. The simulation fit the data relatively well and indicated that the spectrum included the MNP/hydroxymethyl adduct (51%) and the MNP/methyl adduct (24%). The remaining adduct (24%) was best fit by simulating an MNP adduct with a nitrogen splitting of 15.9 G and a hydrogen splitting of 1.3 G. Such a hyperfine pattern is indicative of a carbon-centered radical adduct with one bound

hydrogen (i.e., R$\dot{C}$HR′). This same MNP adduct was also detected when hydrogen peroxide replaced cumene hydroperoxide in the reaction mixture (data not shown). This adduct appears to be derived from P450. Several studies have demonstrated the degradation of P450 heme during reaction with hydroperoxides (*33*−*36*). The heme is degraded into various fragments including methylvinylmaleimide, hematinic acid, and four dipyrrolic propentdyopents (*33*, *34*). Studies using radiolabeled heme have shown that these fragments alkylate the apoprotein (*33*, *35*). Schaefer et al. (*33*) postulated a mechanism for heme degradation by cumene hyroperoxide that included a dipyrrole radical intermediate centered on the meso carbon of the dipyrrolic fragment. Because the meso carbon is allylic (i.e., one hydrogen), a radical centered there could form an adduct with MNP that would have hyperfine characteristics similar to the unassigned MNP adduct in our experiments (i.e., Figures 5D and 6D).

In the absence of O_2, the spectrum obtained with MNP was quite different from that obtained in the presence of O_2. The intensity of the methyl adduct greatly increased, which was in agreement with the increase in the DMPO carbon-centered adduct that was observed under anoxic conditions. This further supported the conclusion that reaction 3 was responsible for producing the DMPO/peroxyl adduct (i.e., DMPO/methylperoxyl). The MNP/hydroxymethyl adduct was also dependent on O_2, as it was not seen in the anaerobic experiment. This result can be explained only if the hydroxymethyl radical was derived from the methylperoxyl radical. Reactions 12 and 13 provide one possibility (*37*, *38*). The methoxyl

$$2CH_3OO^{\bullet} \rightarrow 2CH_3O^{\bullet} + O_2 \qquad (12)$$

$$CH_3O^{\bullet} \rightarrow {}^{\bullet}CH_2OH \qquad (13)$$

radical would then undergo a rearrangement (formally a 1,2 hydrogen shift) to produce the hydroxymethyl radical. The more commonly referenced reaction of primary and secondary peroxyl radicals is the self-terminating reaction proposed by Russell (*39*). Here, two methylperoxyl radicals would combine to form a tetraoxide intermediate that decomposes irreversibly to form methanol, formaldehyde, and singlet O_2.

$$2CH_3OO^{\bullet} \rightarrow CH_3OH + CH_2O + {}^1O_2 \qquad (14)$$

It is possible that the methanol produced in reaction 14 was oxidized by either the cumoxyl or methyl radical (*40*) to yield the hydroxymethyl radical. In either case, the production of the methylperoxyl radical would precede hydroxymethyl radical formation.

The MNP/ethyl radical adduct was also observed under anaerobic conditions. The MNP/ethyl adduct has been observed previously in systems containing the methyl radical and was rationalized by the trapping of the methyl radical twice (*19*, *22*).

Increasing the P450 concentration in the reaction with cumene hydroperoxide resulted in the detection of a strongly immobilized nitroxide. The immobilization of this adduct was reflected by its large nitrogen anisotropy ($2a_{||}^N \sim 61$ G) between the low-field maxima and the high-field minima. The spectrum was indicative of a protein radical and was similar to spectra seen in recent studies involving protein oxidation (*41*, *42*). In these reports it was concluded that the adducts are formed when a radical centered on an amino acid is spin trapped. Therefore, the resulting nitroxide adduct is attached to the protein and tumbles relatively slowly, resulting in the loss of **g-** and **a**-tensor averaging and consequent broadening of the ESR spectrum.

The spin-trapping results presented here definitively demonstrate that ferric P450 can catalyze the homolytic scission of cumene hydroperoxide to initially produce an alkoxyl radical which is capable of diffusing at least some distance from the active site (reaction 2). The production of peroxyl and carbon-centered radicals occurs subsequent to alkoxyl radical formation and primarily involves reactions 11 and 3, although reactions 4 and 5 cannot be excluded. The results are in accordance with several product analysis studies which have also provided evidence that P450 can catalyze the homolytic cleavage of organic hydroperoxides (*10*, *16*, *17*, *43*−*45*).

Alkoxyl radicals such as the cumoxyl radical are very efficient at abstracting hydrogen from polyunsaturated fatty acids, which occurs at a rate of $\sim 2 \times 10^7$ M^{-1} s^{-1} (*46*). Therefore, the results have significance with regard to some confusion in the literature concerning microsomal lipid peroxidation (*9*, *20*, *30*). Our mechanistic conclusions are in agreement with those of Weiss and Estabrook (*9*), who proposed that microsomal lipid peroxidation is a result of the ferric P450- catalyzed, homolytic reduction of cumene hydroperoxide. We did not find that ferrous P450 was required for alkoxyl radical formation as suggested in ref 20, since neither NADPH nor NADPH-P450 reductase were included in any of the reaction mixtures.

It has been argued that alkoxyl radicals are too reactive to diffuse a significant distance from their site of production. Therefore, peroxyl radicals (which are less reactive) have often been thought to be the initiators of lipid peroxidation occurring distal to the site of radical generation (*47*). If this is true, our results would suggest that the methylperoxyl radical (formed by reactions 11 and 3) may be the radical of importance with regard to lipid peroxidation. On the other hand, the highly reactive nature of the cumoxyl radical would make it a candidate for initiating the heme degradation that occurs during the reaction (*33*−*36*).

The heterolytic process produces a two-electron oxidized form of P450 that hydroxylates substrates via the oxygen-rebound mechanism and presumably does not release radicals from the active site (*6*, *7*, *10*). Meanwhile, the homolytic cleavage does produce diffusible radicals. Considering this, we support the view that heterolytic peroxide reduction by P450 is relevant with regard to xenobiotic transformation, while the homolytic mechanism is responsible for the protein degradation and lipid peroxidation that is caused by the P450/hydroperoxide reaction.

References

(1) Hrycay, E. G., and O'Brien, P. J. (1973) Microsomal electron transport. I. Reduced nicotinamide adenine dinucleotide phosphate-cytochrome *c* reductase and cytochrome P450 as electron carriers in microsomal NADPH-peroxidase activity. *Arch. Biochem. Biophys.* **157**, 7−22.

(2) Kadlubar, F. F., Morton, K. C., and Ziegler, D. M. (1973) Microsomal-catalyzed hydroperoxide-dependent C-oxidation of amines. *Biochem. Biophys. Res. Commun.* **54**, 1255−1261.

(3) Nordblom, G. D., White, R. E., and Coon, M. J. (1976) Studies on hydroperoxide-dependent substrate hydroxylation by purified liver microsomal cytochrome P450. *Arch. Biochem. Biophys.* **175**, 524−533.

(4) Griffin, B. W., Marth, C., Yasukochi, Y., and Masters, B. S. S. (1980) Radical mechanism of aminopyrine oxidation by cumene hydroperoxide catalyzed by purified liver microsomal cytochrome P450. *Arch. Biochem Biophys.* **205**, 543−553.

(5) Vatsis, K. P., Deutsch, J., Gelboin, H. V., and Coon, M. J. (1980) Catalytic activity and stereospecificity of phenobarbital-inducible and 5,6-benzoflavone-inducible isozymes of liver microsomal cytochrome P450 in the oxygenation of benzo[*a*]pyrene and *trans*-7,8-dihydroxy-7,8-dihydrobenzo[*a*]pyrene. In *Microsomes, Drug Oxidations, and Chemical Carcinogenesis* (Coon, M. J., Conney, A. H., Estabrook, R. W., Gelboin, H. V., Gillette, J. R., and O'Brien, P. J. Eds.) Vol. II, pp 1065−1080, Academic Press, Inc., New York.

(6) White, R. E., and Coon, M. J. (1980) Oxygen activation by cytochrome P450. *Annu. Rev. Biochem.* **49**, 315−356.

(7) Groves, J. T., and McClusky, G. A. (1976) Aliphatic hydroxylation via oxygen rebound oxygen transfer catalyzed by iron. *J. Am. Chem. Soc.* **98**, 859−861.

(8) Coon, M. J., and Blake, R. C., II (1982) Evaluation of homolytic and heterolytic mechanisms of peroxide oxygen-oxygen bond cleavage by cytochrome P450. In *Oxygenases and Oxygen Metabolism* (Nozaki, M., Yamamoto, S., Ishimura, T., Coon, M. J., Ernster, L., and Estabrook, R. W., Eds.) pp 485−495, Academic Press, Inc., New York.

(9) Weiss, R. H., and Estabrook, R. W. (1986) The mechanism of cumene hydroperoxide-dependent lipid peroxidation: The function of cytochrome P450. *Arch. Biochem. Biophys.* **251**, 348−360.

(10) Thompson, J. A., and Wand, M. D. (1985) Interaction of cytochrome P450 with a hydroperoxide derived from butylated hydroxytoluene: Mechanism of isomerization. *J. Biol. Chem.* **260**, 10637−10644.

(11) Vaz, A. D. N., and Coon, M. J. (1987) Hydrocarbon formation in the reductive cleavage of hydroperoxides by cytochrome P450. *Proc. Natl. Acad. Sci. U.S.A.* **84**, 1172−1176.

(12) Vaz, A. D. N., and Coon, M. J. (1990) Reductive cleavage of hydroperoxides by cytochrome P450. *Methods Enzymol.* **186**, 278−282.

(13) Blake, R. C., II, and Coon, M. J. (1980) On the mechanism of action of cytochrome P450: Spectral intermediates in the reaction of $P450_{LM2}$ with peroxy compounds. *J. Biol. Chem.* **265**, 4100−4111.

(14) Shimizu, T., Murakami, Y., and Hatano, M. (1994) Glu^{318} and Thr^{319} mutations of cytochrome P450 1A2 remarkably enhance homolytic O−O cleavage of alkyl hydroperoxides: An optical absorption spectral study. *J. Biol. Chem.* **269**, 13296−13304.

(15) Lee, W. A., and Bruice, T. C. (1985) Homolytic and heterolytic oxygen−oxygen bond scissions accompanying oxygen transfer to iron(III) porphyrins by percarboxylic acids and hydroperoxides. A mechanistic criterion for peroxidase and cytochrome P450. *J. Am. Chem. Soc.* **107**, 513−514.

(16) Thompson, J. A., and Yumibe, N. P. (1989) Mechanistic aspects of cytochrome P450-hydroperoxide interactions: Substituent effects on degradative pathways. *Drug Metab. Rev.* **20**, 365−378.

(17) Correia , M. A., Yao, K., Allentoff, A. J., Wrighton, S. A., and Thompson, J. A. (1995) Interactions of peroxyquinols with cytochromes P450 2B1, 3A1, and 3A5: Influence of the apoprotein on heterolytic versus homolytic O−O bond cleavage. *Arch. Biochem. Biophys.* **317**, 471−478.

(18) Slaga, T. J., Klein-Szanto, A. J. P., Triplett, L. L., Yotti, L. P., and Trosko, J. E. (1981) Skin tumor-promoting activity of benzoyl peroxide, a widely used free radical-generating compound. *Science* **213**, 1023−1025.

(19) Taffe, B. G., Takahashi, N., Kensler, T. W., and Mason, R. P. (1987) Generation of free radicals from organic hydroperoxide tumor promoters in isolated mouse keratinocytes: Formation of alkyl and alkoxyl radicals from *tert*-butyl hydroperoxide and cumene hydroperoxide *J. Biol. Chem.* **262**, 12143−12149.

(20) Greenley, T. L., and Davies, M. J. (1992) Detection of radicals produced by reaction of hydroperoxides with rat liver microsomal fractions. *Biochim. Biophys. Acta* **1116**, 192−203.

(21) Greenley, T. L., and Davies, M. J. (1993) Radical production from peroxide and peracid tumour promoters: EPR spin trapping studies. *Biochim. Biophys. Acta* **1157**, 23−31.

(22) Chamulitrat, W., Takahashi, N., and Mason, R. P. (1989) Peroxyl, alkoxyl, and carbon-centered radical formation from organic hydroperoxides by chloroperoxidase. *J. Biol. Chem.* **264**, 7889−7899.

(23) Davies, M. J. (1988) Detection of peroxyl and alkoxyl radicals produced by reaction of hydroperoxides with heme-proteins by electron spin resonance spectroscopy. *Biochim. Biophys. Acta* **964**, 28−35.

(24) Barr, D. P., and Mason, R. P. (1995) Mechanism of radical production from the reaction of cytochrome *c* with organic hydroperoxides: An ESR spin trapping investigation. *J. Biol. Chem.* **270**, 12709−12716.

(25) Alterman, M. A., and Dowgii, A. I. (1990) A simple and rapid method for the purification of cytochrome P450 (form LM4). *Biomed. Chromatogr.* **4**, 221−222.

(26) Sandhu, P., Guo, Z., Baba, T., Martin, M. V., Tukey, R. H., and Guengerich, F. P. (1994) Expression of modified human cytochrome P450 1A2 in *Escherichia coli*: stabilization, purification, spectral characterization, and catalytic activities of the enzyme. *Arch. Biochem. Biophys.* **309**, 168−177.

(27) Mair, R. D., and Hall, R. T. (1971) Determination of organic peroxides by physical, chemical, and colorimetric methods. In *Organic Peroxides* (Swern, D., Ed.) pp 535−635, Wiley Interscience, New York.

(28) Duling, D. R. (1994) Simulation of multiple isotropic spin-trap EPR spectra. *J. Magn. Reson.* **104B**, 105−110.

(29) Augusto, O., Beilan, H. S., and Ortiz de Montellano, P. R. (1982) The catalytic mechanism of cytochrome P450: Spin-trapping evidence for one electron substrate oxidation. *J. Biol. Chem.* **257**, 11288−11295.

(30) Cavallini, L., Valente, M., and Bindoli, A. (1983) NADH and NADPH inhibit lipid peroxidation promoted by hydroperoxides in rat liver microsomes. *Biochim. Biophys Acta* **752**, 339−345.

(31) Ingold, K. U. (1969) Peroxy radicals. *Acc. Chem. Res.* **2**, 1−9.

(32) Hanna, P. M., Chamulitrat, W., and Mason, R. P. (1992) When are metal ion-dependent hydroxyl and alkoxyl radical adducts of 5,5-dimethyl-1-pyrroline *N*-oxide artifacts? *Arch. Biochem. Biophys.* **296**, 640−644.

(33) Schaefer, W. H., Harris, T. M., and Guengerich, F. P. (1985) Characterization of the enzymatic and nonenzymatic peroxidative degradation of iron porphyrins and cytochrome P450 heme. *Biochemistry* **24**, 3254−3263.

(34) Guengerich, F. P. (1986) Covalent binding to apoprotein is a major fate of heme in a variety of reactions in which cytochrome P450 is destroyed. *Biochem. Biophys. Res. Commun.* **138**, 193−198.

(35) Yao, K., Falick, A. M., Patel, N., and Correia, M. A. (1993) Cumene hydroperoxide-mediated inactivation of cytochrome P450 2B1. Identification of an active site heme-modified peptide. *J. Biol. Chem.* **268**, 59−65.

(36) Karuzina, I. I., and Archakov, A. I. (1994) Hydrogen peroxide-mediated inactivation of microsomal cytochrome P450 during monooxygenase reactions. *Free Radicals Biol. Med.* **17**, 557−567.

(37) Raley, J. H., Porter, L. M., Rust, F. F., and Vaughan, W. E. (1951) The oxidation of free methyl radicals. *J. Am. Chem. Soc.* **73,** 15−17.

(38) Thomas, S. S., and Calvert, J. G. (1962) The photooxidation of 2,2′ -azoisobutane at 25 °C. *J. Am. Chem. Soc.* **84**, 4207−4212.

(39) Russell, G. A. (1957) Deuterium-isotope effects in the autoxidation of aralkyl hydrocarbons. Mechanism of the interaction of peroxy radicals. *J. Am. Chem. Soc.* **79**, 3871−3877.

(40) Kantrowitz, E. R., Hoffman, M. Z., and Endicott, J. F. (1971) Ultraviolet photochemistry of acetatopentaamminecobalt(III) in aqueous solution. *J. Phys. Chem.* **75**, 1914−1920.

(41) Davies, M. J. (1990) Detection of myoglobin-derived radicals on reaction of metmyoglobin with hydrogen peroxide and other peroxidic compounds. *Free Radical Res. Commun.* **10**, 361−370.

(42) Gunther, M. R., Kelman, D. J., Corbett., J. T., and Mason, R. P. (1995) Self-peroxidation of metmyoglobin results in formation of an oxygen-reactive tryptophan-centered radical. *J. Biol. Chem.* **270**, 16075−16081.

(43) McCarthy, M. B., and White, R. E., (1983) Functional differences between peroxidase compound I and the cytochrome P450 reactive oxygen intermediate. *J. Biol. Chem.* **258**, 9153−9158.

(44) McCarthy, M. B., and White, R. E. (1983) Competing modes of peroxyacid flux through cytochrome P450. *J. Biol. Chem.* **258**, 11610−11616.

(45) Small, R. D., Jr., Scaiano, J. C., and Patterson, L. K. (1979) Radical processes in lipids. A laser photolysis study of *t*-butoxy radical reactivity toward fatty acids. *Photochem. Photobiol.* **29**, 49−51.

(46) White R. E., Sligar, S. G., and Coon, M. J. (1980) Evidence for a homolytic mechanism of peroxide oxygen-oxygen bond cleavage during substrate hdroxylation by cytochrome P450. *J. Biol. Chem.* **255**, 11108−11111.

(47) Marnett, L. J. (1990) Peroxyl free radicals: Biological reactive intermediates produced during lipid oxidation. *Adv. Exp. Med. Biol.* **283**, 65−70.

TX9501501